Welding Process Enhancing Electrodeposition-coating Performance for Ultra-High-Tensile-Strength Steel Sheet

Naohide FURUKAWA*1・Kazuya IKAI*1
*1 Welding Process Department, Technical Center, Welding Business

Abstract

In gas-shield arc-welded joints of ultra-high-tensile-strength steel sheets, there is an issue of increased slag generation, which inhibits electrodeposition-coatability. To address this issue, a welding technology has been developed to reduce the amount of slag generated and improve corrosion resistance after electrodeposition-coating. A welding process has been adopted in which the argon gas ratio in the shielding gas has been increased to 95% (high-argon welding process). The welding consumable has been designed to increase the strength of the welding joint by adding alloying elements that have low affinity with oxygen. In addition, the productivity of welding consumables has also been taken into consideration, and practical application has been sought using composite wires rather than the solid wires that are generally used in the automotive field. This paper describes a welding technology that combines electrodeposition-coatability and fatigue strength, realized by a combination of the welding process and welding consumables.

Introduction

In recent years, the automotive field has seen a growing need for stronger and lighter materials in response to more stringent environmental and collision safety standards. Steel is generally used for automotive suspension parts that support the weight of the chassis. These parts must simultaneously exhibit high fatigue strength, rigidity, and corrosion resistance. To improve the fatigue strength and rigidity of parts with complex shapes, it is necessary to increase the strength of not only the steel sheet but also the welds. Although the thickness of a steel sheet can be reduced if its tensile-strength is increased, a thinner sheet would lead to reaching the fatigue limit sooner if corrosion resistance is not increased. In addition, damage caused by gravel while driving, salt in the atmosphere in coastal regions, and de-icing agents in cold regions necessitate even greater corrosion resistance.

Gas-shield arc welding with solid wire is the typical practice for joining automotive suspension parts. When welding consumables for ultra-high-tensile-strength steel sheets are manufactured using solid wire, the wire strength tends to be high. This is due to work hardening during wire drawing and to the increase in wire hardness from the addition of alloying elements. As a welding consumable, it is necessary for the wire strength to be appropriate for the size of the part for good wire feeding and workability during welding. For wires with a high alloy content, annealing is necessary during drawing to ensure appropriate strength.

Furthermore, multiple stages of annealing may be necessary if the wire strength is not suitable after annealing once. As a result, the wire's productivity is greatly reduced, increasing the cost. Therefore, Kobe Steel set out to develop a welding consumable designed for 980 MPa-grade steel sheet using composite wire. The design of the material accounts for formability during wire manufacturing, with a mild steel outer layer and flux with alloying elements as the core. **Table 1** shows the advantages and disadvantages of composite versus solid wire. For high-strength materials that are difficult to draw, composite wire is advantageous because it is both economical and has a higher deposition rate.

One disadvantage of composite wire is low rigidity, which tends to reduce the straightness of the wire slightly. This aspect was evaluated by testing weldability at a part manufacturer's facility. This paper introduces welding technology that results in welding joints with excellent corrosion resistance and fatigue strength, even in the welding of ultra-high-tensile-strength steel by using the composite wire and welding process described above.

Table 1 Advantages and disadvantages of composite wire against solid wire

		Solid wire	Composite wire
Typical cross section			
Formability	Mild steel	○	○
	High tensile steel	○	◎
Production cost	Mild steel	○	△
	High tensile steel	○	◎
Deposition rate		○	◎
Wire stiffness		○	△

[Judge standard] ◎: Better - ○:Standard - △:Poor - ×:Bad

1. Underlying technology

1.1 Concept behind improving corrosion resistance

Our concept behind improving corrosion resistance is divided into the welding process and the subsequent electrodeposition-coating process, as shown in **Fig. 1**. In gas-shield arc welding, typical shielding gas compositions are 100% CO_2 or an 80/20 blend of Ar with CO_2 to prevent the incorporation of atmosphere into the molten metal. CO_2 dissociates into CO and O under the arc. Oxygen stabilizes the arc but is an active gas that combines with Si, Mn, and other alloying elements, producing slag. Oxide slag containing silicon as the main constituent is highly insulative, so if this composition of slag is on the surface of the weld bead, a coating film will not form during the electrodeposition-coating process after welding. Therefore, the amount of slag on the weld bead must be minimized to improve electrodeposition-coatability.

To overcome this challenge, we employed a high-argon welding process that uses a shielding gas of a 95/5 blend of Ar with CO_2 to stabilize the arc during welding while reducing active gas, thereby suppressing slag formation[1]. There is an established method for the subsequent electrodeposition-coating process in which the viscosity of the electrodeposition-coating is decreased to increase fluidity during baking, thereby coating the insulative material[2].

Our concept is to minimize slag using a high-argon welding process and then thicken the electrodeposition-coating to increase the amount of fluid coating and cover the slag in the uncoated areas.

1.2 Welding consumables

It is possible to reduce slag by using a high-argon welding process with a higher inert gas ratio. Various related efforts have been pursued to reduce slag and improve electrodeposition-coatability in welding consumables[3)~5)].

Two approaches have been proposed for welding consumables used in combination with a high-argon welding process to achieve low-slag welding. The optimal conditions for each approach are a point of study. **Table 2** shows the approaches to reducing slag in a high-argon welding process by coordinating the welding consumables to processing conditions.

The first approach is to suppress slag formation by increasing the ratio of inert gas, concentrate, and recover the slag, and transport the slag to the weld end. Concentrated slag detaches easily; as a mechanism to concentrate slag, the welding wire contains 0.020% sulfur. Adding sulfur changes the convection of the molten pool, causing microscopic slag particles to aggregate in the crater during welding and be transported along with the arc. Another factor, aside from molten pool convection, that influences slag behavior is the flow rate of the shielding gas. Reducing the gas flow rate helps concentrate slag and transport it to the weld end in a stable way[5]. Therefore, it is best to use a nozzle with a larger diameter than normal. Wire for gas-shield arc-welding that imparts the above-mentioned characteristics to slag is called "slag-concentrating wire" in this paper. The second approach to reducing slag is to transport slag to the rear of the molten pool and actively incorporate it into the Fe-based oxide film in a deconcentrated state. Welding consumables for this approach contain Ti, which forms oxides with higher liquidus temperatures than those of Si and Mn oxides. Compared with Si and Mn, Ti forms molten slag that is higher in temperature and therefore more strongly affected by the flow of the plasma, providing the driving force for the molten slag to move rearward in the molten pool. To incorporate slag transported to the rear of the molten pool into the Fe-based oxide film, it is best to expose slag to the atmosphere from the area near the solid-liquid interface at the rear of the molten pool. According to Yamasaki et al.[5], a high welding speed or a nozzle diameter smaller than a certain value results in a region of the weld bead without slag after welding. Changing these two parameters

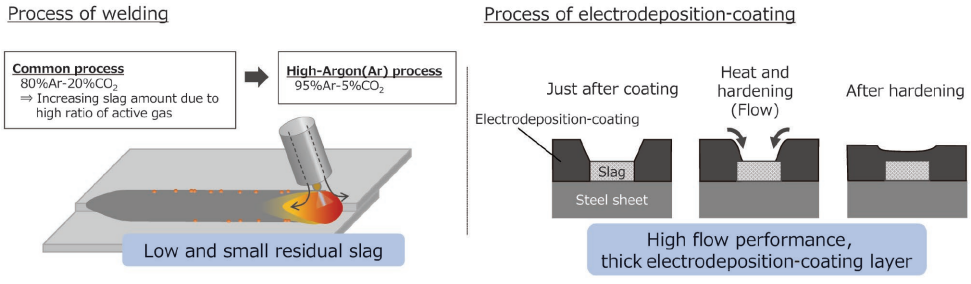

Fig. 1 Basic idea to improve corrosion resistance

Table 2 Two approaches for slag reduction method

Welding process	High−Ar process	
Shielding gas	95%Ar-5%CO_2	
Wire type	Slag concentrating	Slag deconcentrating
Unique chemical composition in wire	S add.	Ti add.
Gas flow rate	20 (Liter/min.)	
Size of nozzle	Φ19 (mm)	Φ13(mm)
Welding speed	Normal	Faster
Schematic drawing	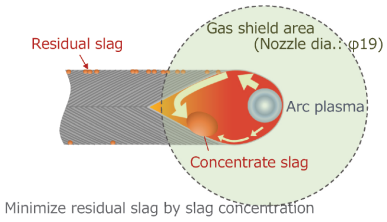 Minimize residual slag by slag concentration	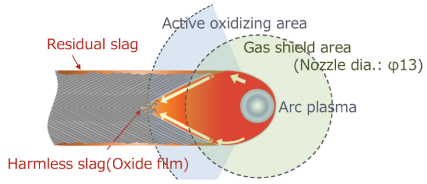 Creating harmless slag by active oxidizing in the rear molten pool
Observation by HSV	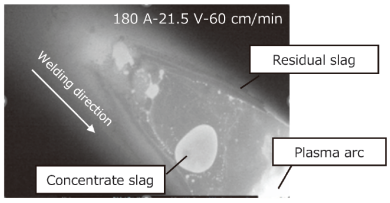	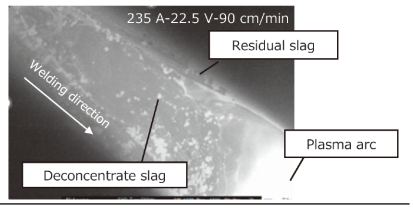

Table 3 Corrosion resistance performance of lap weld joint

Welding process	Conventional MAG	High −Ar process	
Shielding gas	100%CO_2 or 80%Ar-20%CO_2	95%Ar-5%CO_2	
Wire type	Normal YGW12	Slag concentrating	Slag deconcentrating
Base metal	440 MPa-grade steel, 2.0 mm^t		
Bead appearance after electrodeposition-coating	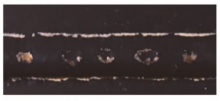	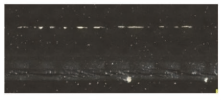	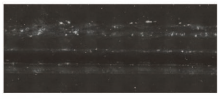
Bead appearance after 10 cycles of corrosion test	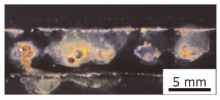		
Judge*	3	4	5

* [Judge standard] 5(Good) − 4(better) − 3(Standard) − 2(poor) − 1(Bad)

accordingly increases the area of the molten pool exposed to the atmosphere and promotes more aggressive coating by the Fe-based oxide film. This is a more sensible approach, as the welding speed can be increased without increasing porosity due to air entrainment or reducing mechanical performance. In this paper, gas-shield arc welding wire that deconcentrates slag as described above is called "slag-deconcentrating wire."

Table 3 shows welding joints in 440 MPa-grade steel after electrodeposition-coating and corrosion testing as described below. Compared with conventional metal active gas (MAG) welding, welding joints produced using the high-argon welding process exhibit significantly better electrodeposition-coatability. Additionally, in comparing the two approaches to reducing slag, the slag-concentrating wire shows some rusting from residual slag that could not be fully concentrated. By contrast, the slag-deconcentrating wire has good corrosion resistance if the slag is properly deconcentrated and rendered harmless.

Since an increase in slag is expected in welding wire for ultra-high-tensile-strength steel, we decided to design a welding wire based on slag-deconcentrating wire because of its demonstrated higher corrosion resistance.

2. Welding technology for ultra-high-tensile-strength steel

2.1 Welding consumables

In developing a welding wire for ultra-high-tensile-strength steel sheet, we investigated a composite wire that combines a mild steel strip with excellent formability as the outer layer and a mixed flux with alloying elements as the core.

Table 4 shows the target chemical compositions of the trial wires when fully melted. Alloys are added to 980 MPa-grade steel sheet to achieve the required strength. The weld metal is affected by the base metal composition and the alloy composition of the wire. A high alloying content inevitably increases slag when welding ultra-high-tensile-strength steel sheet. To minimize slag in the welding wire, we considered using carbon or Cr to improve the strength of the weld metal instead of Si, which has a high affinity with oxygen. Carbon has little effect on the amount of slag because it combines with oxygen and vaporizes as CO_2. Cr has a relatively low affinity with oxygen. When alloying elements with a higher affinity are present, Cr is not readily oxidized and consumed in the slag-metal reaction. Therefore, Cr will bond with oxygen only to a limited degree and will mostly remain in the weld metal.

2.2 Experiment conditions

2.2.1 Welding and electrodeposition-coating

For the trials, we lap welded 980 MPa-grade steel sheets provided by Mazda Motor Corporation in a horizontal welding position. **Table 5** and **Fig. 2** show the welding conditions. The image of slag on the weld bead was binarized for calculation of the area ratio of slag. The welding joints were cleaned, degreased, prepared, conversion coated (zinc phosphate), and cleaned again before coating with black cationic electrodeposition-coating (target thickness 20 μm). Images of the coated surfaces were binarized for calculation of the non-coated area.

2.2.2 Combined cyclic corrosion test (CCT)

CCT is a method for accelerated testing of the corrosion resistance of metal materials, coatings, and platings. This test method involves repeated corrosion cycles of salt spray, drying, and wetting in a test chamber. We evaluated the corrosion resistance of lap weld joints, selecting specimens from joints using trial wires A-F for their low slag and good electrodeposition-coatability. Specimens were subjected to up to 50 cycles of the testing conditions stipulated in JASO M609 (Japanese Automotive Standards Organization) to definitively reveal the difference in corrosion resistance between trial wires. We took images of the specimens to record their corrosion status after removing them from the test chamber.

2.2.3 Fatigue testing of welding joints

Specimens were prepared by performing electrical discharge machining on pieces welded under the conditions in Table 5. Bending fatigue tests were performed on the specimens with a stress ratio R = 0. The benchmark was wire of specification JIS Z 3312 G43A2M 16, which is commonly used as a welding consumable for 440 to 780 MPa-grade steel sheets. **Table 6** shows the fatigue test conditions.

Table 4 Typical chemical compositions of trial wires for 980 MPa-grade steel

Wire	C	Si	Mn	Cr	Ti	Ni, Mo	Ceq.
Wire A	0.08	0.29	1.45	0.10	0.14	Add.	0.54
Wire B	0.09	0.14		0.13			0.55
Wire C	0.09	0.04		0.13			0.54
Wire D	0.08	0.29		0.10	0.10		0.54
Wire E	0.09	0.14		0.13			0.55
Wire F	0.09	0.04		0.13			0.54

[JIS/WES] Ceq.: C+Mn/6+Si/24+Ni/40+Cr/5+Mo/4+V/4

Table 5 Welding condition for lap weld joint

Welding robot	DAIHEN Almega AX-V6
Power source	DAIHEN Digital Pulse DP400R
Shielding gas	95%Ar-5%CO_2, 20 ℓ/min
CTWD	15 mm
Nozzle inner dia.	13 mmφ
Torch angle	45°
Base metal	980MPa-grade steel, thickness : 2 mm
Current (Voltage)	240 A (24.5 V)
Welding speed	110 cm/min

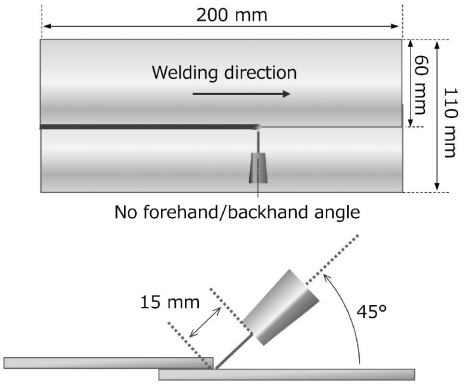

Fig. 2 Wire aiming position when lap weld joint done

Table 6 Bending fatigue test condition

Test temperature	RT
Stress ratio	R≒0 (pulsating fatigue test)
Frequency	25 Hz
Number of cycles to failure	2×10^6 cycles or 10% less than initial torque

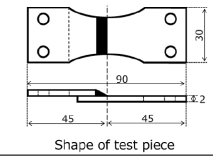

Shape of test piece

2.2.4 Hardness testing of welding joints

Vickers hardness testing was performed on cross-sectional macro specimens of welding joints from the same specimens from which the fatigue test samples were taken. Hardness was measured at the lower side weld toe, an area that can affect the fatigue strength of the welding joint, in an area spanning the weld metal, heat-affected zone, and base metal. The load for hardness measurement was 3 N.

2.3 Experiment results and explanation

2.3.1 Results of evaluating slag generation and electrodeposition-coatability

Table 7 shows the weld beads after lap welding and electrodeposition-coating. **Figs. 3** and **4** show quantitative results as calculated by image analysis in the form of the area ratio of slag and the non-electrodeposition-coated area. These results show that there is less residual slag on the bead with a lower ratio of Ti and Si, which are strong deoxidizing elements. A comparison of the beads after electrodeposition-coating confirms that most of the bead, including the residual slag, was electrodeposition-coated. Wires A-C (0.14% added Ti) exhibited good electrodeposition-coatability even on the upper side of the bead where there was residual slag. Conversely, wires D - F (0.10% added Ti), which had a relatively low amount of slag, exhibited poor electrodeposition-coatability in some areas. In summary, although good electrodeposition-coatability was achieved even with a high amount of residual slag, there were cases in which electrodeposition-coatability was insufficient even with a low amount of slag.

2.3.2 Results of slag analysis

We examined the cross-sections of the slag, focusing on the residual slag on the upper side of the beads, which exhibited differing degrees of electrodeposition-coatability. Specifically, we used electron probe microanalysis (EPMA) to perform elemental mapping and COMPASS multivariate image analysis software (Thermo Fisher Scientific Inc.) to perform phase separation analysis.

Fig. 5 shows the ratios of the main oxides that make up the slag as calculated based on the elements

Table 7 Bead appearance after welding and after electrodeposition-coating

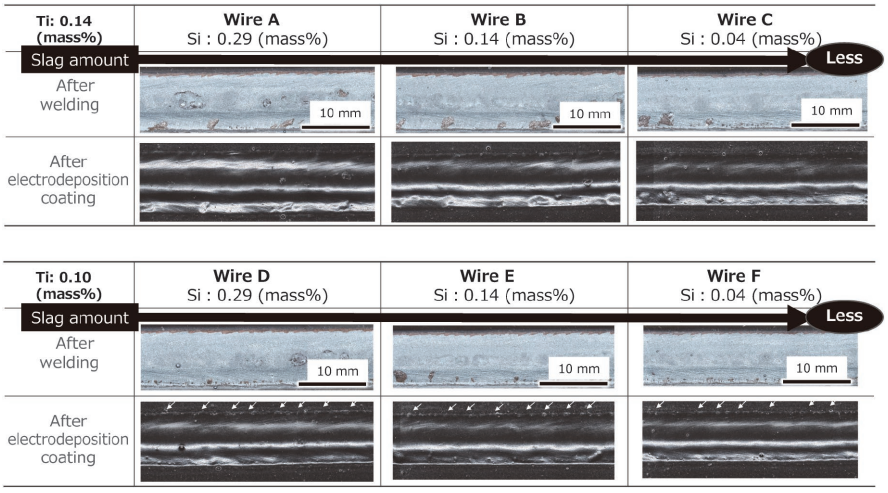

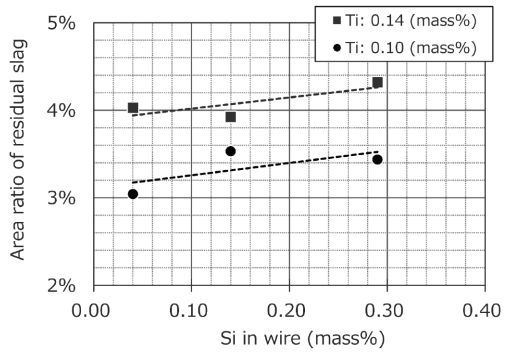

Fig. 3 Area ratio of residual slag

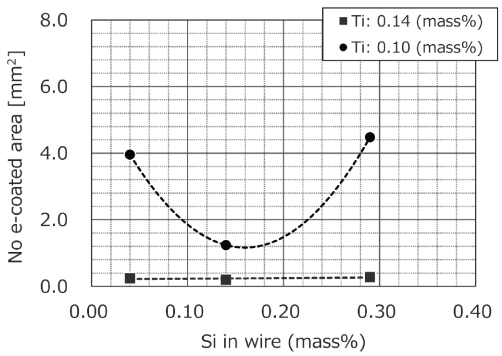

Fig. 4 Non- electrodeposition-coated area

and mass ratios identified by element mapping. While the ratio of SiO_2 in the slag tends to decrease as the ratio of Si in the wire decreases, no significant differences were observed in the ratios of TiO_2, MnO, or other components.

Table 8 shows the distribution of the oxide phase as output by COMPASS. Phases with a ratio of 20% or more in the slag were extracted. Components constituting 10% or more of a phase were deemed representative components of those phases. The Mn-Ti-Si oxide and Mn-Ti oxide phases were found to be main phases of the slag in every case. As the Si content in the wire decreases, the Mn-Ti oxide phase tends to precipitate in the form of dendrites from the bottom of the slag (steel ground side) to the top (electrodeposition-coating ground side). Additionally, the boundary between phases is generally distinct. This tendency is stronger in the slag of wires A - C (0.14% added Ti), which have good electrodeposition-coatability.

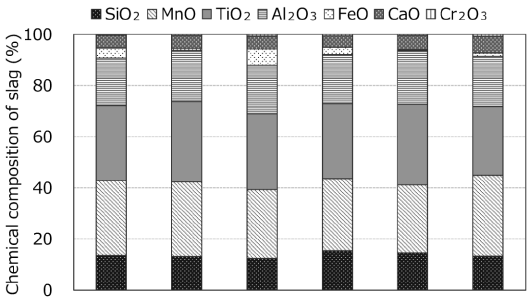

Ti in wire (mass%)	0.14			0.10		
Si in wire (mass%)	0.29	0.14	0.04	0.29	0.14	0.04

Fig. 5 Percentage of slag elements taken from upper side in the welding bead

This can be explained by assuming that the Mn-Ti oxide phase is more conductive than the Mn-Ti-Si oxide phase. It seems that the conductive pathways take a complex three-dimensional path from the bottom of the slag up, fostering good electrodeposition-coatability despite an increase in the area ratio of the slag. Quantitative analysis of the conductivity of each oxide phase is a potential future research area to elucidate the mechanisms behind improving electrodeposition-coatability.

2.3.3 Results of the CCT

Table 9 shows the CCT results for 980 MPa-grade steel sheet upon application of a cationic electrodeposition-coating to a lap weld fillet joint created with wire B. This joint exhibited superior

Table 8 Phase analyzed results at cross-sectional slag

Wire	Wire A	Wire B	Wire C	Wire D	Wire E	Wire F
Ti in wire (mass%)	0.14			0.10		
Si in wire (mass%)	0.29	0.14	0.04	0.29	0.14	0.04
Composition image	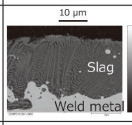	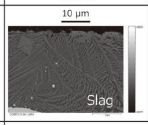	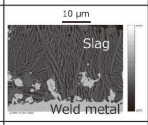	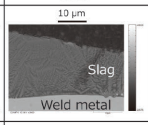	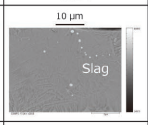	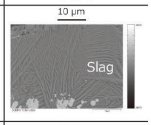
Mapping image	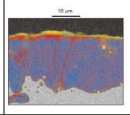	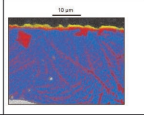	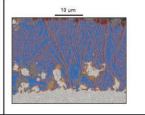	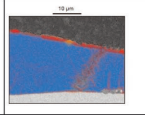	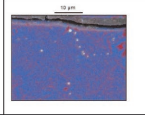	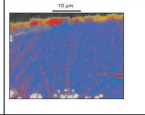
Slag component phase	Mn-Ti-Si Mn-Ti Fe-Mn-Ti Others (Fume etc.)	Mn-Ti-Si Mn-Ti Others (Fume etc.)	Mn-Ti-Si Mn-Ti Fe-Mn-Ti	Mn-Ti-Si Mn-Ti Fe-Mn-Ti	Mn-Ti-Si Mn-Ti	Mn-Ti-Si Mn-Ti Others (Fume etc.)

Table 9 CCT results of weld joint prepared with Wire B

Welding process	High-Ar process	
Wire type	Conventional wire for high-tensile-strength-steel (Slag concentrating)	Wire B for ultra-high-tensile-strength-steel (Slag deconcentrating)
Base metal	440 MPa-grade steel, 2.0 mm^t	Wire B 980 MPa-grade steel, 2.0 mm^t
After welding	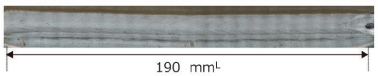 190 mm^L	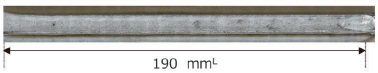 190 mm^L
AFter electrodeposition coating	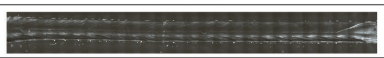	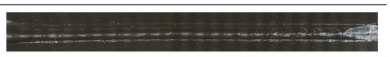
After 30 cycle of CCT		
After 50 cycle of CCT	N/A	

*Conventional wire: G43A2M 16

electrodeposition-coatability in comparison with the joint created using conventional wire and 440 MPa-grade steel sheet. Furthermore, after 50 cycles of the CCT, no rust originating from the residual slag on the weld bead was observed, confirming that the material has good corrosion resistance.

2.3.4 Results of fatigue testing of welding joints

Fig. 6 shows the fatigue test results of lap fillet weld joints. Introduced here are the fatigue properties of wire B, which balances electrodeposition-coatability and weld metal strength in the welding of 980 MPa-grade steel sheet.

Testing shows improved fatigue properties of the welding joint when conventional wire is paired with 980 MPa-grade steel sheet in comparison with 440 MPa-grade steel sheet.

The combination of wire B and 980 MPa-grade steel sheet is shifted toward a higher number of cycles to failure compared with conventional wire under the same stress amplitude. Further, the fatigue strength of the former at 2 million cycles is about 1.5 times higher.

Table 10 shows the macro-level cross-sections of the lap weld fillet joints and the toe radii and flank angles. While the geometry of the weld toe greatly affects the fatigue properties of the lap fillet weld joint, there were no significant differences in this feature with the trial wire used in this study. Therefore, it is concluded that the increase in the tensile-strength of the steel sheet and weld metal increases the load-bearing capacity of the welding joint itself, thus increasing fatigue strength.

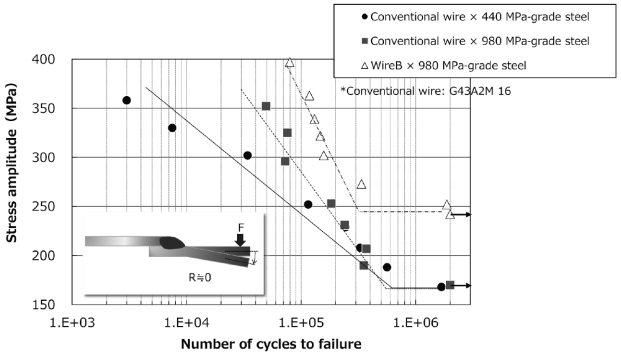

Fig. 6 Fatigue strength of lap fillet weld joint

2.3.5 Results of hardness testing of the weld metal

Fig. 7 shows the results of the Vickers hardness test near the lower-side weld toe of the welding joint. The weld metal of the welding joint using conventional wire is harder in combination with the 980 MPa-grade steel sheet in comparison with the 440 MPa-grade steel sheet. This could be because the base metal is diluted by alloying elements added to the 980 MPa-grade steel sheet. The hardness of

Table 10 Cross-section of lap fillet weld joint

	Conventional wire × 440 MPa-grade steel	Conventional wire × 980 MPa-grade steel	WireB × 980 MPa-grade steel
	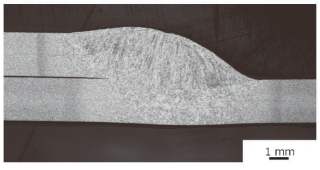	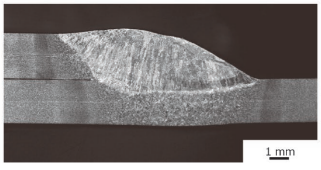	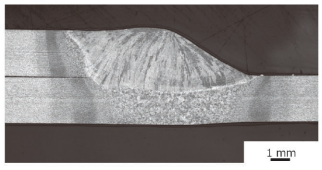
Frank angle (°)	150	149	152
Toe radius (mm)	2.0	1.6	2.1

*Conventional wire: G43A2M 16

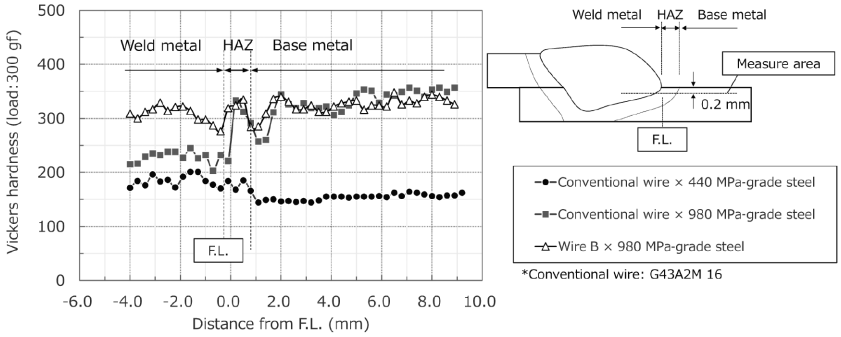

Fig. 7 Vickers hardness around lower side weld toe

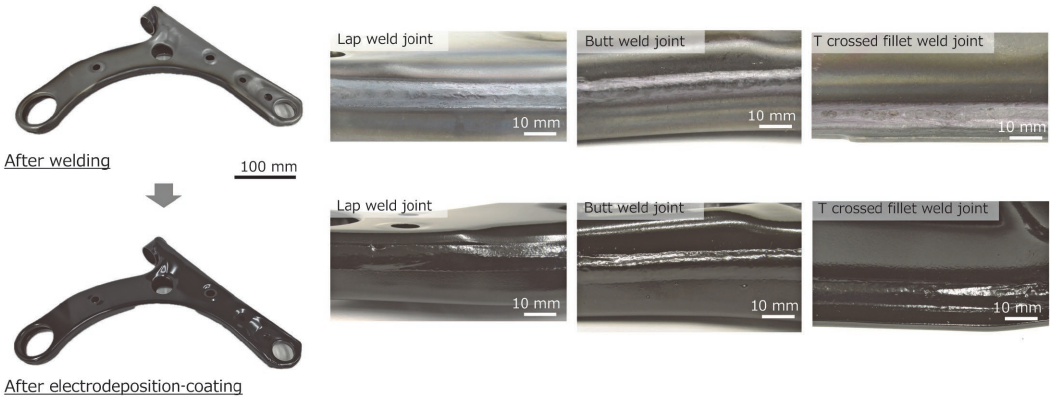

Fig. 8 Trial Lower Control Arm and bead appearance at unique welding position

the weld metal of the welding joint using wire B, which exhibited the best results in the plane bending fatigue test, is approximately HV 300.

In summary, increasing the hardness of the weld metal near the toe, which is subject to concentrated stress, is an effective means of improving the fatigue properties of lap fillet weld joints.

3. Application to actual parts

Since wire B exhibited excellent corrosion resistance and fatigue strength in laboratory tests, we evaluated its weldability and electrodeposition-coatability on actual parts. Specifically, we conducted testing on a lower control arm made from 980 MPa-grade steel sheet (thickness 2 mm^t). This steel, produced by Mazda Motor Corporation, reduces component weight by approximately 25% compared with parts made from conventional 780 MPa-grade steel sheet.

Fig. 8 (top) shows the lower control arm and its main welds, created using wire B. Good weldability was confirmed for the three types of joints required for this part, namely, butt welds, lap welds, and T-crossed fillet welds. One drawback of composite wire is its low rigidity, causing concerns regarding wire target performance during robot welding; however, defect-free weld beads were achieved. Fig. 8 (bottom) shows the lower control arm after cationic electrodeposition-coating. The wire has good electrodeposition-coatability, and the expected effects of combining slag-deconcentrating wire with a high-argon welding process have been confirmed in actual parts.

Conclusions

Ultra-high-tensile-strength steel sheets are being developed to reduce the thickness of automotive suspension parts and thereby reduce vehicle weight. Adding alloys to steel sheet to increase tensile-strength also increases slag, which interferes with electrodeposition-coatability. Perforation caused by rust reduces the functional life of thin steel sheet. To overcome these challenges, we developed a high-argon welding process technology that increases strength while reducing slag and improves corrosion resistance through alteration of the slag. In selecting welding consumables for high-tensile-strength steel, we chose composite wire for its productivity and procurement cost. In the automotive field, although stainless steel composite wire has been used for exhaust system parts, it is almost never used for suspension parts. The component manufacturers that made application of our composite wire possible rated it highly in terms of weldability and productivity. We anticipate that this development will be recognized as a solution technology for reducing the weight of vehicle bodies in the automotive field and that the scope of use will expand. We will continue to bring a green society to fruition through our joining technology.

Finally, we would like to express our sincere appreciation to Mazda Motor Corporation and Yorozu Corporation for their collaboration in this joint development, including in the evaluation of corrosion resistance, weldability, and durability of actual parts.

References

1) M. Tanaka et al. Mazda Technical Review. 2017, No.34, pp.123-124.
2) M. Tanaka et al. Mazda Technical Review. 2018, No.35, pp.27-28.
3) R. Suzuki et al. R&D Kobe Steel Engineering Reports. 2017, Vol.66, No.2, pp.64-66.
4) H. Kinashi et al. R&D Kobe Steel Engineering Reports. 2023, Vol.72, No.1, pp.81-82
5) R. Yamasaki et al. R&D Kobe Steel Engineering Reports. 2019, Vol.69, No.1, pp.98-104.